Journal of Alloys and Compounds 488 (2010) 430–436

Contents lists available at ScienceDirect

Journal of Alloys and Compounds

journal homepage: www.elsevier.com/locate/jallcom

# Coating of Al substrate by metallic Ni through mechanical alloying

R. Pouriamanesh [a,*], J. Vahdati-Khaki [a], Q. Mohammadi [b]

[a] Department of Materials Science and Metallurgy, Faculty of Engineering, Ferdowsi University of Mashhad, Azadi Square, P.O. Box 91775-1111, Mashhad, Iran
[b] Department of Materials Science and Metallurgy, Faculty of Engineering, Shahid Bahonar University of Kerman, Kerman, Iran

ARTICLE INFO

*Article history:*
Received 30 May 2009
Received in revised form 30 August 2009
Accepted 31 August 2009
Available online 8 September 2009

*Keywords:*
Mechanical Alloying
Intermetallic
Coating
Microstructure
Scanning electron microscopy
SEM

ABSTRACT

Aluminum alloy substrate was coated by nickel powder using mechanical alloying (MA) method. Aluminum samples, which were ball-milled with nickel powder in a planetary ball-mill, were in the cubic form with 1 cm × 1 cm × 1 cm dimensions. During the mechano-activation processing, the substrate surface was impacted by some flying balls along with particles of powder. The substrate surface was hardened and activated as a result of the high-energy impact of balls. Ni–Al intermetallic phases were formed in the coating layer. Formation of such intermetallic phase increases the local temperature. The increased temperature causes a better adherence of the nano-sized coating to the substrate. Coated samples were annealed at 550 °C for 330 min. The measurements of Vickers microhardness were performed on both substrate and coating. The microstructure of samples was investigated by scanning electron microscopy (SEM) and optical microscope. Chemical composition was analyzed by energy dispersive X-ray spectroscopy (EDS). The final structure was studied by X-ray diffraction (XRD) analysis. Transmission electron microscopy (TEM) was also used to observe coating particles.



## 1. Introduction

Mechanical surface coating of aluminum alloys has attracted a great deal of attention recently. Many elements have been used and investigated for surface alloying of aluminum materials. Nickel is an interesting element because it can form a number of intermetallic compounds with Al. If there are a sufficient number of Ni–Al intermetallic precipitates suitably dispersed, there can be a significant improvement in the hardness [1]. A variety of coating techniques on metal plates have been established, including cement-packing, thermal spraying, hard facing, laser cladding, etc. [2–7]. Recently, it has been understood that mechanical alloying (MA) can be utilized as a flexible method to coat objects [8–10] in order to obtain nano-scale surface layers [3,10–12].

Fig. 1 shows a schematic illustration of the process. The principle of the method is for a substrate and powder to be placed into a rotary chamber along with a number of steel balls [9,13]. When some powder is processed by using MA, part of the milled powder forms a coating film over the milling balls and on the inner wall of the container [8,14]. Due to repeated substrate-to-ball collisions, the powder particles become cold-welded to the surface [13]. Frequent impact of balls has been also used to treat [15,16], activate and harden the surface [17]. In MA method, coarse-grain structure of surface was refined as well as the grains of powder. Surface treated-structure can modify the properties of the surface of materials [10]. It has been demonstrated that ultrafine grains could accelerate diffusion [3,18–20] and chemical reactions on the surface [3,21,22]. Activation of substrate and deposition of coating [9] powder take place simultaneously. The surface, being activated, promotes chemical reaction and the bonding between target and powder. The particles, fractured, provide large interface area; therefore reactions between the components become possible. Chemical interaction, diffusion [3,23], alloying, and the formation of new phases, takes place at the interface between the target and the coating particles [17]. Chemical changes may take place during a post-annealing step or during the deposition process itself. If deposition of a uniform coating on a section of the container wall is desired, it is necessary to have spatially uniform distribution of impacts [15].

Surface alloying of metal plates by using MA has been investigated by a number of researchers. Romankov et al. [10,24] showed that MA method can be used for the fabrication of Ti–Al coatings. Their experiments resulted in Ti + Al coating with a thickness of 200 μm and Al coating with a thickness of 50 μm after milling for 2 h at room temperature. The surface morphology of these coatings was very rough; therefore they did an annealing process. Different aluminide phases were produced on the samples during annealing. Zhan et al. [21] investigated Fe–Al intermetallic coatings on steel. Coatings of Fe–Al with thickness of 17 μm for 15 min and 90 μm for 120 min were produced at 560 °C treatment. The nanostructure of these coatings consisted mainly η-$Fe_2Al_5$ with small amounts of θ-$FeAl_3$ and β-FeAl. Torosyan et al. [17] investigated

* Corresponding author. Tel.: +98 5118763305; fax: +98 5118763305.
*E-mail address:* rpouria2000@gmail.com (R. Pouriamanesh).

0925-8388/$ – see front matter © 2009 Elsevier B.V. All rights reserved.
doi:10.1016/j.jallcom.2009.08.150

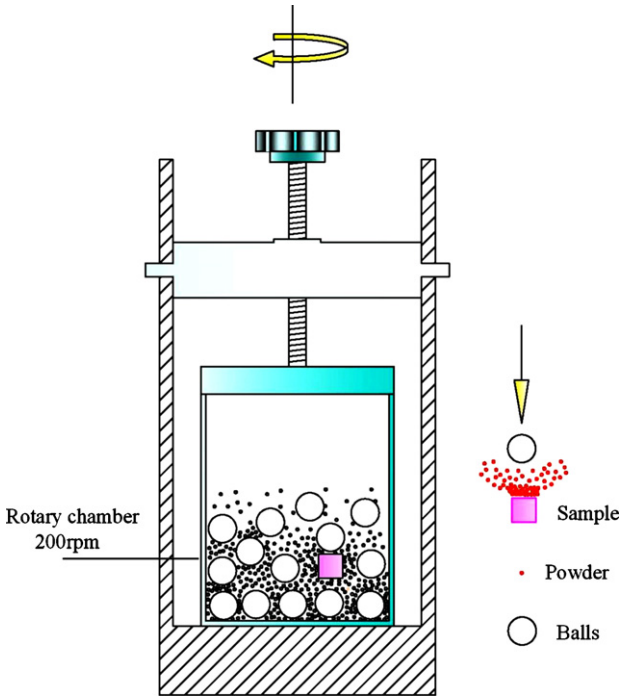


**Fig. 1.** Schematic illustrations of MA process.

$WO_3$ and PbO coatings on Al (6061 alloy) substrate. Takacs et al. [15] coated substrate of steels with Al powders and Al substrate with Ni powders. Furthermore, the method has been successfully used for depositing hard coatings such as TiN and TiC/TiN on different substrates [25,26]. Korsunsky et al. [27] investigated low-friction coatings such as Mo + S and carbon–diamond like carbon (C–DLC) on titanium alloy substrates. They fabricated the well-adhered dry film lubricating layers with a significant improvement in the tribological characteristics.

However, there are limited studies on the formation of Ni coating on Al substrates using MA. Hence in this context, Ni metallic powder was coated on Al substrate using MA. The produced coatings were characterized by X-ray diffraction (XRD), optical microscopy, scanning electron microscopy (SEM), dispersive X-ray spectroscopy (EDS), and transmission electron microscopy (TEM).

## 2. Experimental

Ni powders were coated on Al substrate by means of MA. The starting materials were 1 g Ni (>99.5%, <10 μm) powder and pure Al (>99%) as a cubic bulk sample. A small amount of ethanol was added to prevent excessive welding of the powders to the steel balls and the container. 8 chromium steel balls (6 balls-0.95 cm diameter and 2 balls-1.27 cm) were used. The ball-to-powder ratio was 39 in mass. The milling process was carried out in an ambient atmosphere. A planetary ball-mill with a 200 rpm rotating speed was selected (Fig. 1). In order to prevent contamination by the atmosphere, milling chamber was completely sealed; if the container is not properly sealed, the atmosphere surrounding the container leaks into the container and contaminates the powder. When the chamber is properly sealed, interstitial contaminants can be reduced to a minimum at the milling stage [13]. The milling times were 20, 50, 80, 120, 200, 300, 420, 720, 1080 and 1500 min. Some coating samples were annealed at 550 °C for 330 min in Ar atmosphere and later furnace was cooled down to room temperature.

After milling, the samples were cut with a refine saw and then polished. The coating thickness was measured from all sample sides using optical and SEM microscopy and the average thickness was calculated for each sample.

The resulting structure was studied using X-ray diffraction (XRD) analysis (Cu Kα). The cross-section microstructure was characterized with a LEO 1450VP microscope by scanning electron microscopy (SEM) equipped with energy dispersive spectrometry analysis (EDS). The samples were coated with thin layer of gold deposited by sputtering process for SEM investigations.

The composition was analyzed by using energy dispersive X-ray spectroscopy (EDS) using Link System (Oxford Instruments, Central Laboratory of Ferdowsi University of Mashhad, Iran). Transmission electron microscopy (TEM) with a LEO 912AB with an operating voltage of 120 kV was also performed. For transmission electron microscopy (TEM) investigations, a liquid polymer resin was coated on specimen surface. The resin was dried in air and then detached from the surface. This polymer (replica) contains small particles of coating. The replica was solved in a specific solvent to separate the particles from polymer. The separated particles were studied in TEM.

The Ni grain size ($D$) was determined using the Scherrer formula:

$$D = \frac{k\lambda}{\beta \cos\theta} \quad (1)$$

where $k$ is a constant and generally assumed to be 0.89, $\lambda$ the wavelength of Cu Kα radiation, $\theta$ half of the diffraction angle, and $\beta$ is the width of half height for the (1 1 0) diffraction peak of Ni. The measurements of Vickers microhardness for both

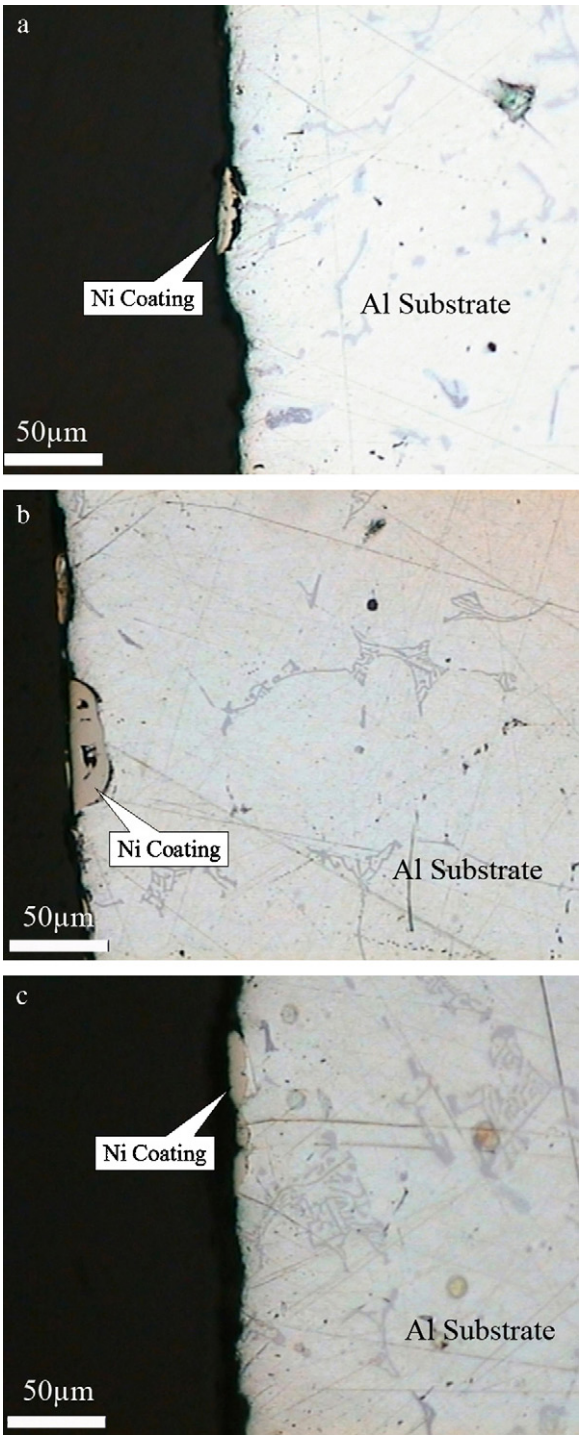


**Fig. 2.** Optical micrograph of the cross-section of aluminum substrate coated with Ni, after (a) 20 min, (b) 50 min, and (c) 80 min milling.

coating and substrate were performed using a Buehler microhardness tester under a load of 25 g for 20 times and the average was used to ensure obtaining a reasonably representative value. All indents were kept away from porous locations. As the measurements carried out in the cross-section of the coating, indents were always positioned not less than 50 μm away from the surface or the interface between the substrate and the coating.

## 3. Results and discussion

Fig. 2 shows the cross-section microstructure of coatings which were produced at the initial milling time intervals. At these times, Ni powder was adhered to substrate in some places. By further milling the balls could sweep together; therefore, a few amounts of Ni particles were inserted into the surface of the substrate. While coating the balls with a layer of Ni powders, the balls collide with each other and they transfer the powders to the Al substrate; consequently, mixings and reactions between Al and Ni begin [17]. Cold welding between particles and substrate under repeated ball collisions led to formation of a composite coating [10].

Fig. 3 shows the cross-section microstructure and coating composition on Al substrate after different milling times. Scanning

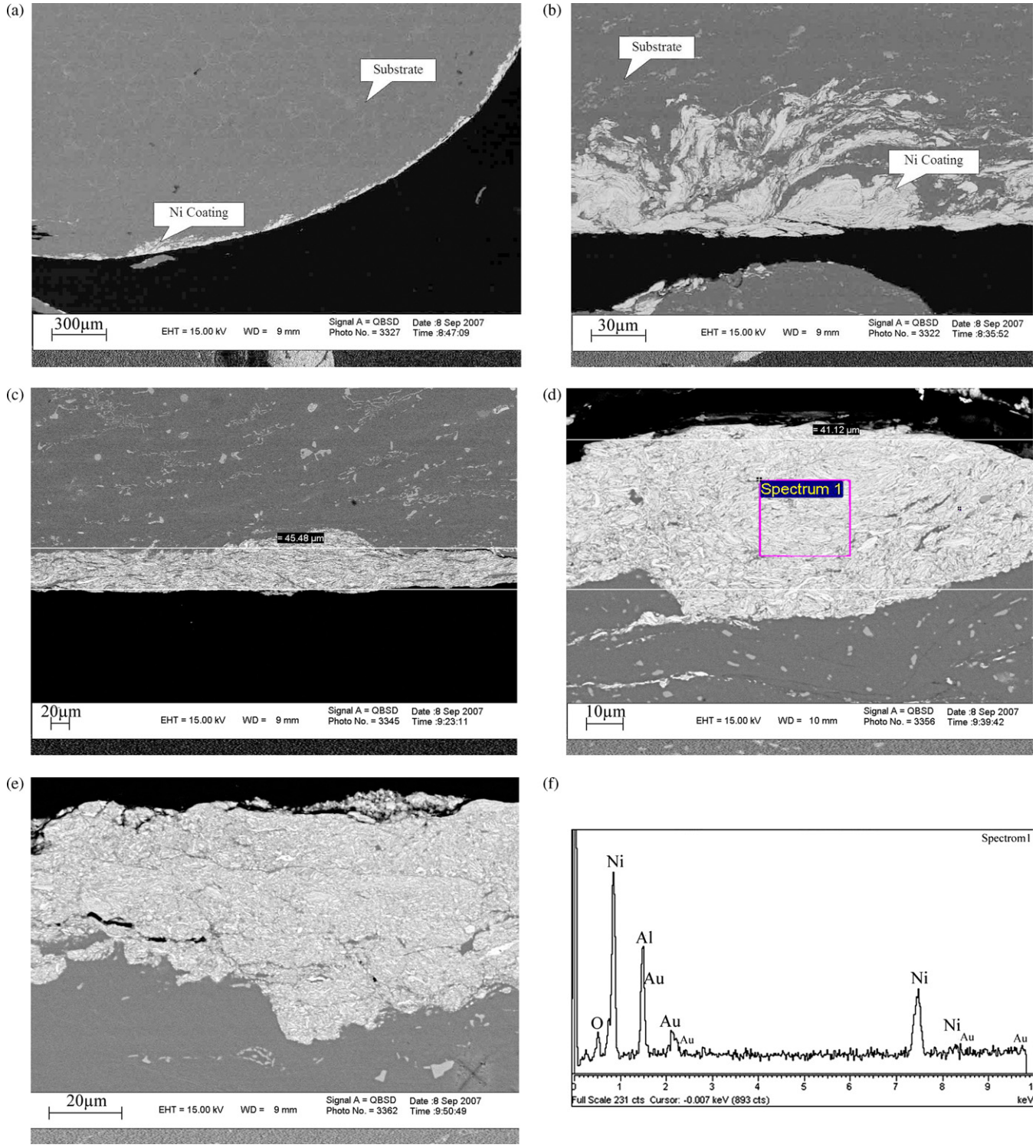


**Fig. 3.** SEM micrographs of the cross-section of MA-coatings after (a and b) 120 min, (c) 300 min, (d) 420 min, (e) 720 min of milling, and (f) EDS of (d).

electron microscopy (SEM) images show the formation of a thick layer of coating on the substrate. The Ni–Al coating formed very rapidly when the milling duration was between 80 and 120 min (Figs. 2 and 3). It should be noted that the substrate underwent plastic deformation under the ball collisions and its surface became slightly bent; this can be seen in Fig. 3a. The coating deposited at the 200 min of milling exhibited rough layer-like morphology, implying that the Ni–Al mixture covered the substrate layer-by-layer (Fig. 3b). Ni coating mixed with the aluminum plate in layers, folding and shifting over each other are due to ball collisions. Ni flowed into the pores between Al particles as a result of ball collisions on the Al substrate; therefore, a dense Al + Ni coating was grown. The as-synthesized coating in Fig. 3c showed a structure with high apparent density and free of porosity and cracks and good adherence to substrate.

Cold welding caused non-uniformity on the samples. Cold welding occurred in the early stages of mechanical alloying (MA), when the Ni particles were soft and their tendency to weld was high [10]. During mechanical alloying (MA), cold welding was restrained [10]. The powder particles and Al substrate became harder and more brittle and started to flake and smooth due to the ball collisions. During MA a layered structure with a clear separation between Ni and Al begins to develop near the top surface, as shown in Fig. 3e. The formation of a layered structure implies that plastic deformation increased at further milling times [13]. The cracks, which are shown in Fig. 3e, propagate to the coating layer and substrate; therefore, coating particles and fragments of Al plate would fracture and detach. Detached fragments of Al can be mixed mechanically with powders and being attached to the substrate.

Fig. 3f is spot analysis (EDS) of coating layer which shows Ni and Al elements. The EDS spectrum also shows Au peaks due to metallic gold that was sputter coated on the samples surface to reduce electrical charging during SEM measurements.

Material of the grinding medium, such as Fe, was not detected in the top coating layer; the balls and chamber inner walls were likely coated by a Ni–Al layer in the early stages of the MA processing, which prevented the release of Fe into the coating [10,13]. The magnitude of contamination during MA depends upon the milling time and intensity, nature of the powder, ball-to-powder weight ratio, seal integrity, etc. (see Ref. [23] for examples). In mechanical alloying, the chamber should be properly sealed to prevent continuous leaking from outside. If the container is not properly sealed, the atmosphere surrounding the container leaks into the container and contaminates the powder [13].

The microstructure near the surface was refined by the plastic deformation in the ball-milling process [21]. With the employed method, ball collisions, which caused a large amount of structure defects [3,13,18,20–23] and local high temperatures at the collision zones, resulted in severe plastic deformation of the substrate [21]. Based on Zhan's investigations [21], it was understood that the temperature at the collision zones may have risen above the melting point of Al (660 °C), therefore, reaction between Ni and Al promotes and Ni–Al intermetallic compounds are formed.

Fig. 4, measured by optical and SEM images, shows the coating thickness of samples. The mean thickness of Ni coating ranged from 10 to 100 μm for initial millings. The coating thickness was 100 μm in some places at 420 min of milling. The mean coating thickness increased to its maximum value at 420 min of milling and gradually decreased thereafter with further increases of milling time (Fig. 4). Milling for 1080 min reduced the coating thickness; however, the coating surface became smoother. At this time the lamellae near the surface were totally fractured and those in the middle area of the coating were flattened. It is obvious that the compressive pressure propagated through the coating and modified the structure across the coating with time [13]. However, further increases in milling duration may result in breaking the coating due to the development

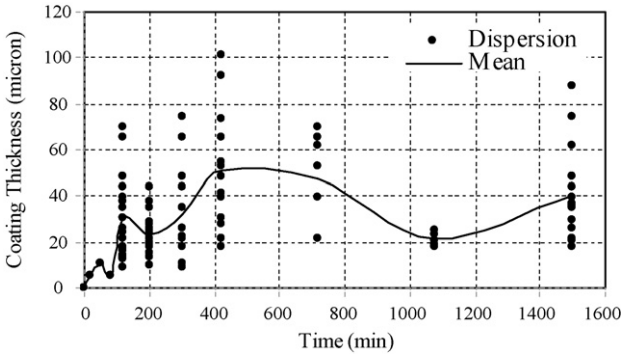


**Fig. 4.** Coating thickness of samples at various milling times.

of cracks in the highly deformed top area (Fig. 3e). The dispersion of coating thickness at each milling time revealed that it is difficult to produce a uniform coating compared with either chemical vapor deposition (CVD) or physical vapor deposition (PVD). The uniformity of coating thickness in our process may have been as a result of choosing different and proper experimental conditions. More detailed studies on the uniformity of coating thickness are subject to further investigations.

The reaction between the Al substrate and the Ni powder can be investigated by XRD. Fig. 5 shows the XRD spectra of coating surface, treated before and after heat treatment at different milling times, indicating the phase evolution of the coatings as a function of milling times. The XRD patterns show the presence of both elemental Ni and Al constituents with small amounts of $Ni_3Al$, $Al_3Ni$, NiO and NiAl. The intensity of Ni–Al intermetallic compounds is too little in as-milled samples. The intermetallic phases were existed at the beginning of the process. The existence of intermetallic phases revealed that reaction between Al substrate and Ni powders are initiated. During heat treatment, on the surface of the sample, different aluminide phases were formed as a result of interdiffusion and reaction between Ni and Al. After heat treatment, mentioned peaks appeared with higher intensity than as-milled samples.

Ni grain size in coating could be estimated from the XRD patterns. As it is shown in Fig. 6, the Ni grain size, estimated by Scherrer formula, decreased sharply and was about 9 nm at 720 min milling. The most aggregation of intermetallic phases were at 420 min milling time in samples which undergone heat treatment. In compare with as-milled samples, the broadened main peaks were narrowed; therefore, Ni grain size was increased. As a result Ni grain size was about 20 nm at 1500 min in milling.

The formations of Ni–Al intermetallic compounds, which are reported in Table 1, are exothermic. The exothermic heat led the temperature to increase above the Al melting point; therefore, Al substrate may have melted locally. The melted Al could move through pores in the coating layer because of capillary effect; in addition the melted Al may have reacted with Ni coating through a self-propagating high-temperature synthesis (SHS) reaction [28]. Heat treatment may be extended to the coating layer in order to join the substrate firmly [28]. Diffusion of Ni and Al atoms took place at the interface of Ni coating and the initial alloy layer especially after heat treatment as shown in Fig. 7.

Substrate outward surface grains were refined by ball collisions and the substrate inward grains had a coarse-grain structure. The inward diffusion of Ni atoms may have been restrained. The inward diffusion of Ni, which is much slower than the grain boundary diffusion, is lattice controlled. This effect slowed down the inward growth of Ni-rich phases, leaving Al atoms diffuse through the alloy layer along the high-density grain boundaries, and resulted in outward growth of the Ni-rich phases. Thus, existence of Al in coating

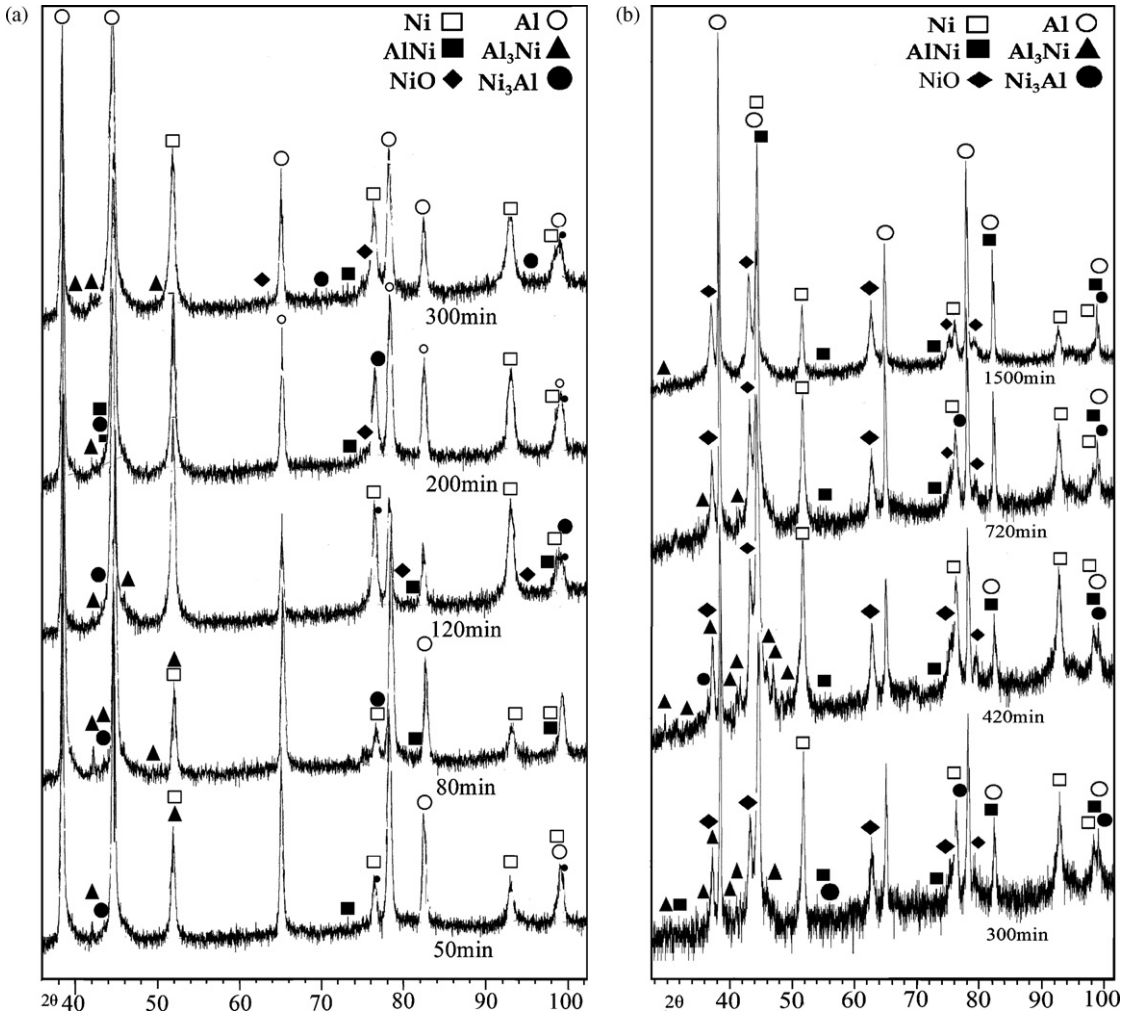


**Fig. 5.** X-ray diffraction patterns (Cu Kα) of MA-coatings: (a) as-milled samples and (b) after anneal.

layer, as is shown in EDS analysis may have happened because of the following reasons:

1. Detachment of substrate because of ball collisions and mixing mechanically with milled powders.
2. Diffusion of Al through coating layer.
3. Melting of Al locally and its movement through pores in the coating layer because of capillary effect.

**Table 1**
Formation enthalpie Ni–Al intermetallic components.

| Component | $Ni_3Al$ | $Al_3Ni$ | NiAl |
|---|---|---|---|
| $\Delta H_{f(298\,^\circ C)}$ (J mol$^{-1}$) | −153.134 | −150.624 | −118.407 |

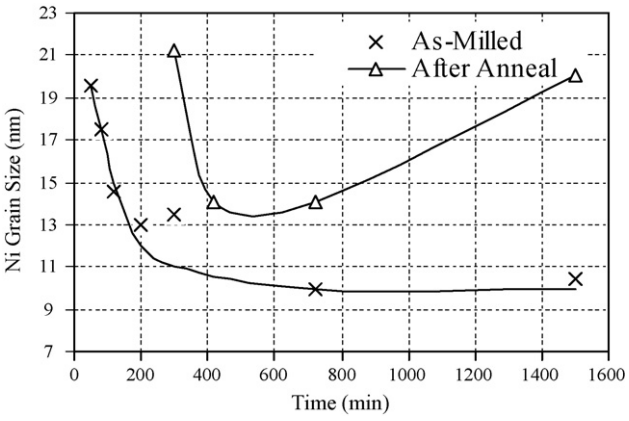


**Fig. 6.** Ni grain size in coating layer measured by Sherrer Formula.

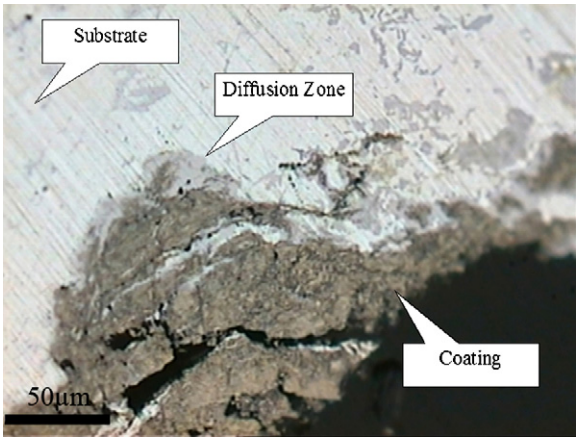


**Fig. 7.** Annealed coating at 550 °C for 330 min.

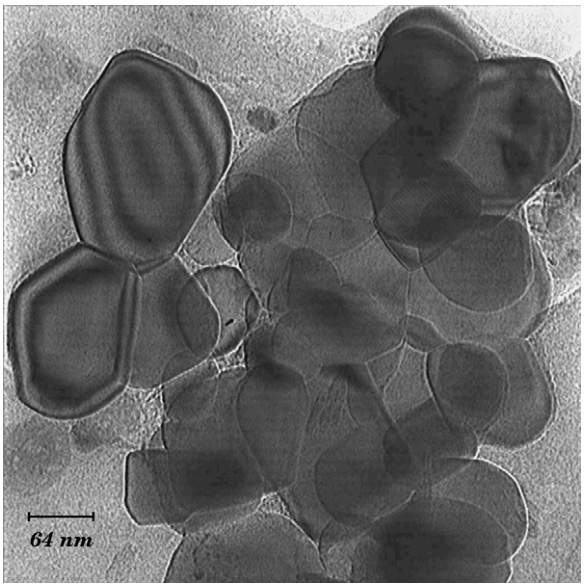


**Fig. 8.** TEM image of coating layer after 300 min milling.

The TEM micrograph in Fig. 8 shows the nano-size of coating particles. Considerable refinement and reduction of particles size into the nanometer scale at the top surface layer of the Ni–Al coating with increase of milling duration is evident from the TEM observation. With subsequent increase of milling duration more energy was transferred to the particles, particles were flattened, the surface area for contact was increased and the diffusion process was enhanced. The size of particles in the coating layer ranged from 5 to 100 nm. This experience shows that the ball collisions were uneven in all directions and the coated particles were welded together during milling.

The coating particles, as are shown in Fig. 8, contain particles stuck to the sample surface by mechanical force at the last step of milling process; besides, for some of these particles cold welding has not been completed yet. Subsequently, these coating particles were able to preserve the primitive spherical morphology and some of these particles may be the early Ni powders.

Fig. 9 shows the Vickers microhardness tests of the coating and the substrate. The evolution of Vickers hardness can be correlated qualitatively to the evolution of yield stress in the present alloy, e.g. the higher the hardness, the higher the yield stress [29]. Fig. 10 shows the hardness variations which have been measured by micro-Vickers hardness tester around the substrate and coating. The microhardness of all coating layers was higher than the substrate ones because of the existence of Ni–Al intermetallic compounds. When the impact of balls resulted in straining, the hardness increased, and when the impact of balls resulted in detachment of

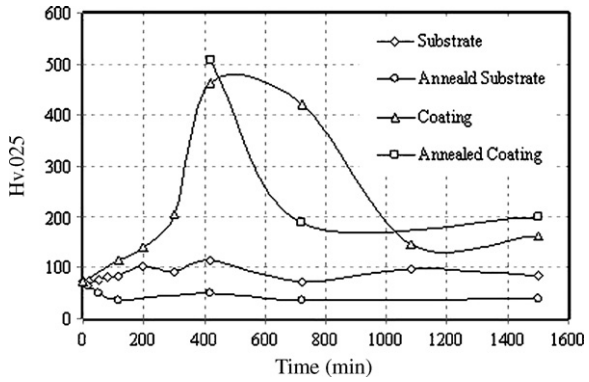


**Fig. 10.** Microhardness of substrate and coating: (a) as-milled and (b) annealed at 550 °C for 330 min.

substrate, the hardness decreased. Straining produced a high density of dislocations [13]. Fig. 9b shows the effect of hardness, having been resulted with straining, along the center of the substrate; therefore hardness decreased.

Here are some reasons of increasing the hardness of material consisted both substrate and coating layer:

a) The refined structure of substrate and coating as a result of the impact of balls.
b) The enhanced grains in surface of substrate and coating.
c) The existence of Ni–Al intermetallic compounds in material.

The variation of microhardness at this paper is within good agreement with previous experimental and theoretical investigations. Hot pressed $Ni_3Al$ samples, prepared using MA, had value of Vickers hardness of 427 as Meng et al. [30] reported, and NiAl sprayed samples had 440 Hv as Wang et al. [31] reported. In this paper the value of microhardness of coating, which was within good agreement with previous researches, was 427 Hv at 420 min milling in as-milled samples. Decreasing of microhardness of coating after 420 min milling in as-milled samples may be related to the existence of more Al in coating layer than the previous times.

Heat treatment resulted in softening of the material including both the substrate and the coating. The microhardeness of the substrate, which ranged from 35 to 70 Hv (Fig. 10), is significantly reduced during heat treatment, but the value of microhardness of coating, which was more than as-milled samples, ranged from 464 to 548 Hv at 420 min milling. Increasing of Hv in heat treatment samples can be related to high density of Ni–Al intermetallic compounds in as much as XRD patterns showed. The microhardness of coating decreased in both the as-milled and the heat treatment samples because of the Ni grain growth or the more existence of Al than previous times in coating layer after 420 min milling.

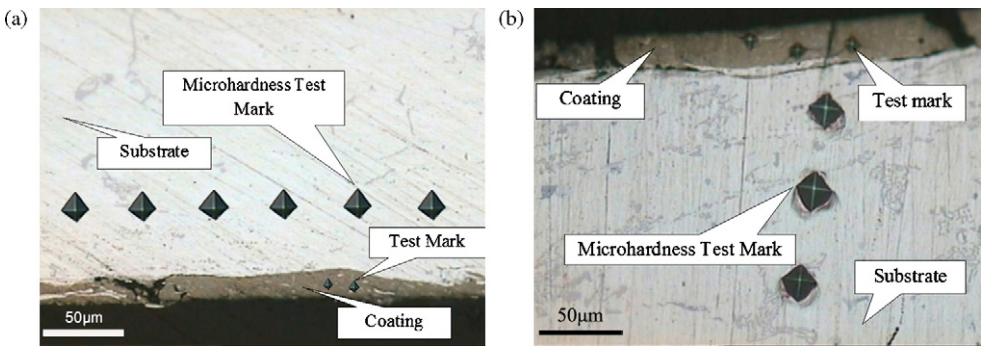


**Fig. 9.** Microhardness of substrate and coating of samples: (a) 420 min milling and (b) 1500 min milled and anneled at 550 °C for 330 min.

## 4. Conclusion

Formation of Ni–Al nano-sized coating on Al substrate is possible through MA. The Ni–Al intermetallic components formed in coating layer. Further studies are needed to achieve a better understanding to produce a uniform coating. EDS analysis showed Al and Ni elements in coating layer. The existence of Al in coating layer was due to the detachment of substrate, diffusion of Al and melting of Al. The examination of coating hardness showed high value of hardness because of Ni–Al intermetallic, straining and modified structure of coating.

## Acknowledgments

The authors express their thanks to the metallogeraphy laboratory and central laboratory of Ferdowsi University of Mashhad for their cooperation in this investigation. This work was supported in part by Pare-Tavoos research institute. The help of Dr. Aghasi Torosyan for his kind considerations is greatly appreciated. We would also like to thank Dr. Yousefi for his helps in XRD test.

## References

[1] M. Heydarzadeh, Process. Technol. 118 (2001) 187–192.
[2] Y. Wang, W. Chen, L. Wang, Wear 254 (2003) 350–355.
[3] H. Lee, S. Lee, H. Shin, K. Ko, J. Alloys Compd. 478 (2009) 636–641.
[4] K.A. Khor, Y. MurakoshP, M. Takahashi, T. Sano, Mater. Process. Technol. 48 (1995) 413.
[5] S.B. Mishra, K. Chandra, S. Prakash, B. Venkataraman, Mater. Lett. 59 (2005) 3694.
[6] J. Gang, O. Elkedimc, T. Grosdidier, Surf. Coat. Technol. 190 (2005) 406.
[7] B.Q. Wang, S.W. Lee, Wear 239 (2000) 83–90.
[8] L. Takacs, A.R. Torosyan, J. Alloys Compd. 434–435 (2007) 686.
[9] S. Romankov, S.D. Kaloshkinc, Y. Hayasakad, Zh. Sagdoldinab, S.V. Komarove, N. Hayashia, E. Kasaia, J. Alloys Compd. 483 (2009) 386–388.
[10] S. Romankov, W. Sha, S.D. Kaloshkin, K. Kaevitser, Surf. Coat. Technol. 201 (2006) 3235.
[11] Z.B. Wang, N.R. Tao, W.P. Tong, J. Lu, K. Lu, Acta Mater. 51 (2003) 4319.
[12] N. Tao, H. Zhang, J. Lu, K. Lu, Mater. Trans. 44 (2003) 1919.
[13] S. Romankov, S.D. Kaloshkin, Y. Hayasaka, S.V. Komarov, N. Hayashi, E. Kasai, J. Alloys Compd. 484 (2009) 665–673.
[14] Á. Révész, L. Takacs, J. Alloys Compd. 441 (2007) 111.
[15] L. Takacs, Á. Révész, Chem. Sust. Dev. 15 (2007) 231–235.
[16] ASTM Standard B695-04, Standard Specification for Coatings of Zinc Mechanically Deposited on Iron and Steel (2004).
[17] A. Torosyan, L. Takacs, J. Mater. Sci. 39 (2004) 5491–5496.
[18] W. Gao, Z. Liu, Z. Li, Adv. Mater. 13 (2001) 1001.
[19] Z. Liu, W. Gao, K. Dahm, F. Wang, Acta Metall. Mater. 46 (1998) 1691–1700.
[20] W. Gao, Z. Li, Y. He, Mater. Sci. Forum 369 (372) (2001) 579.
[21] Z. Zhan, Y. He, D. Wang, W. Gao, Intermetallics 14 (2006) 75.
[22] B. Bhushan, X.D. Li, Int. Mater. Rev. 48 (2003) 125.
[23] C. Suryanarayana, Prog. Mater. Sci. 46 (2001) 1.
[24] S. Romankov, A. Mamaeva, S.D. Kaloshkin, S.V. Komarov, Mater. Lett. 61 (2007) 5288.
[25] S. Romankov, S.V. Komarov, E. Vdovichenko, Y. Hayasaka, N. Hayashi, E. Kasai, Int. J. Refract. Met. Hard Mater. 27 (2009) 492–497.
[26] S. Romankov, Y. Hayasaka, E. Vdovichenko, S.V. Komarov, N. Hayashi, E. Kasai, Surf. Coat. Technol. 203 (2009) 1879–1884.
[27] A.M. Korsunsky, A.R. Torosyan, K. Kim, Thin Solid Films 516 (2008) 5690.
[28] H.Y. Lee, A. Ikenaga, S.H. Kim, K.B. Kim, Intermetallics 15 (2007) 1050–1056.
[29] J. Lapin, S. Wierzbinski, T. Pelachova, Intermetallics 7 (1999) 705–719.
[30] J. Meng, C. Jia, Q. He, J. Alloys Compd. 421 (2006) 200–203.
[31] Y. Wang, W. Chen, Surf. Coat. Technol. 183 (2004) 18–28.